Functional integrity of thalamocortical circuits differentiates normal aging from mild cognitive impairment.

Jose L. Cantero, Mercedes Atienza, German Gomez-Herrero, Abel Cruz-Vadell, Eulogio Gil-Neciga, Rafael Rodriguez-Romero, David Garcia-Solis

▶ **To cite this version:**

Human Brain Mapping

WILEY

Functional integrity of thalamocortical circuits differentiates normal aging from mild cognitive impairment.

scholarONE™
Manuscript Central

Functional integrity of thalamocortical circuits differentiates normal aging from mild cognitive impairment

Jose L. Cantero[1*], Mercedes Atienza[1], German Gomez-Herrero[2], Abel Cruz-Vadell[1],

Eulogio Gil-Neciga[3], Rafael Rodriguez-Romero[4], David Garcia-Solis[5]

[1]Laboratory of Functional Neuroscience, Network for Biomedical Research in Neurodegenerative Diseases (CIBERNED), University Pablo de Olavide, Seville, Spain

[2]Department of Signal Processing, Tampere University of Technology, Tampere, Finland

[3]Dementia Unit, Neurology Department, University Hospital Virgen del Rocio, Seville, Spain

[4]Neuroradiology Unit, Radiodiagnostic Department, University Hospital Virgen del Rocio, Seville, Spain

[5]Nuclear Medicine Department, University Hospital Virgen del Rocio, Seville, Spain

[*]**Correspondence to:**

Jose L. Cantero, Ph.D.
Laboratory of Functional Neuroscience
University Pablo de Olavide
Ctra. de Utrera, Km. 1
41013-Seville, Spain

Phone: + 34 954 977433
Fax: + 34 954 349151
Email: jlcanlor@upo.es

Running title: Neurodegeneration effects on thalamocortical circuits

Abstract

Resonance in thalamocortical networks is critically involved in sculpting oscillatory behavior in large ensembles of neocortical cells. Neocortical oscillations provide critical information about the integrity of thalamocortical circuits and functional connectivity of cortical networks, which seem to be significantly disrupted by the neuronal death and synapse loss characterizing Alzheimer's disease (AD). By applying a novel analysis methodology to overcome volume conduction effects between scalp electroencephalographic (EEG) measurements we were able to estimate the temporal activation of EEG-alpha sources in the thalamus and parieto-occipital regions of the cortex. We found that synaptic flow underlying the lower alpha band (7.5-10 Hz) was abnormally facilitated in patients with mild cognitive impairment (MCI) as compared to healthy elderly individuals, particularly from thalamus to cortex (~38% higher). In addition, the thalamic generator of lower alpha oscillations was also abnormally activated in MCI patients. Regarding the upper alpha subdivision (10.1-12.5 Hz), both controls and MCI patients showed a bidirectional decrease of thalamocortical synaptic transmission which was age-dependent only in the control group. Altogether, our results suggest that functional dynamics of thalamocortical networks differentiate individuals at high risk of developing AD from healthy elderly subjects, supporting the hypothesis that neurodegeneration mechanisms are active years before the patient is clinically diagnosed with dementia.

Introduction

MCI is characterized by subtle but clinically significant memory loss beyond what is expected from normal aging. This clinical condition seems to represent a transitional stage between normal aging and some prevalent neurodegenerative disorders such as Alzheimer's disease (AD) [Petersen et al., 1999]. From a neuropathological perspective, the density of neuritic plaques [Sabbagh et al., 2006; Markesbery et al., 2006; Price and Morris 1999] and neurofibrilary tangles [Guillozet et al., 2003] characterizing AD also become apparent in the neocortex of MCI patients. Unfortunately, these instigators of neuronal damage can only be empirically identified in postmortem studies, which make them worthless in clinical practice as early markers of AD.

Cognitive symptoms present in AD are mostly caused by massive cell death and synaptic loss mainly affecting association areas and the pyramidal cells that supply the long projections among distant neocortical regions [Morrison and Hof, 1997]. This scenario results in a global disruption of local and long-range neural circuits that are revealed by changes in brain oscillations recorded with the electroencephalogram (EEG). EEG measurements emerge from summated excitatory and inhibitory postsynaptic potentials primarily generated by synaptic activity of large pyramidal neurons [Lopes da Silva and Van Rotterdam, 1993]. Among EEG oscillations, the alpha rhythm has been reported to be typically affected in AD patients [Huang et al., 2000; Osipova et al., 2005; Babiloni et al., 2006]. Alpha waves are intrinsically generated by synaptic networks of neocortical pyramidal neurons in layer 5 by means of the tonic activation of N-methyl-D-aspartate receptors with endogenous glutamate [Silva and Connors, 1991]. The neuronal damage evident in diverse neocortical regions of MCI patients [Sabbagh et al., 2006; Markesbery

et al., 2006; Price and Morris, 1999; Guillozet et al., 2003] may indeed affect both the intrinsic mechanism of oscillatory behavior observed in layer 5 neurons and the cluster formation of microscopic neural sources involved in the cortical generation of the human alpha rhythm [Silva and Connors, 1991].

The thalamus plays a crucial role in the generation of alpha rhythm by means of intrinsic mechanisms [Hughes et al., 2004] and dynamical interactions of thalamocortical networks [Lopes da Silva, 1991]. Studies in AD patients have found amyloid deposits and neurofibrillary tangles in the thalamus [Rudelli et al., 1984; Masliah et al., 1989; Braak and Braak, 1991] as well as a significant loss of its gray matter [Karas et al., 2004] that was correlated with impaired cognitive functioning [de Jong et al., 2008]. These findings are not surprising given the role of the thalamus in declarative memory [de Rover et al., 2008; Van der Werf et al., 2003], and postulate a mild involvement of this subcortical structure in neurodegenerative processes.

The human alpha response of the thalamus occurs earlier than that of the cortex [de Munck et al., 2007]. This finding highlights the relevance of *in vivo* techniques to determine cause-effect relationships between the neural generators of this cerebral rhythm. Damage of cortical pyramidal cells and thalamic neurons might underlie synaptic dysfunctions affecting the reciprocal communication between thalamus and cortex during the generation of alpha rhythm even in the preclinical stages of AD. This hypothesis was tested in the present study by evaluating the integrity of functional connectivity between thalamic and neocortical EEG sources of alpha oscillations in both healthy aged persons and amnesic MCI patients. To achieve this goal, the most prevalent independent sources of spontaneous EEG-alpha activity were estimated after removing the volume conduction

4

effects from EEG recordings. A novel methodology based on multivariate autoregressive (MVAR) modeling and Independent Component Analysis (ICA) [Gómez-Herrero et al., 2008] was able to reliably determine the temporal activation of the EEG alpha sources and their approximate intracerebral locations. Causal relationships between the neural sources of EEG-alpha rhythm were estimated by using measurements of functional directionality based on Granger causality [Kaminski et al., 2001], and the significance of directional strength evaluated with surrogated data. Since previous evidence has shown that the presence of the allele ε4 in the apoliprotein E (ApoE) not only increases the risk of developing AD [Caselli et al., 2007; Wang et al., 2002; Corder et al. 1993] but also correlates with changes in the cortical dynamics of alpha rhythm [Babiloni et al., 2006], both probability of source activation and direction of synaptic flow between EEG-alpha sources were compared between carriers and non-carriers of the allele ε4 in controls and MCI groups.

Methods

Subjects

Twenty MCI patients (9 females, mean age: 66.8 ± 4.7 yr) and 20 cognitively normal volunteers (10 females, mean age: 68.4 ± 6.1 yr) were recruited from the local community and the Dementia Unit of the Neurology Service at the University Hospital Virgen del Rocio, respectively. MCI patients and control subjects were matched in educational years and handedness. Demographics and neuropsychological profile of healthy elderly and MCI groups are shown in Table 1. All participants provided signed informed consent

before any testing. Study protocols were previously approved by the Ethical Committee for Clinical Investigations at the University Hospital Virgen del Rocio, and the Ethical Committee for Human Research at the University Pablo de Olavide.

The diagnosis of MCI was based on consensus criteria [Petersen et al., 1999]: (i) subjective memory complaints confirmed by the informant (ii) objective memory decline on neuropsychological tests evidenced by scores $\geq$ 1.5 standard deviations below the age-appropriate mean, (iii) clinical dementia rating (CDR) global score of 0.5 (questionable dementia), (iv) normal independence function both judged clinically and by means of a standardized scale for the activities of daily living, and (v) not meeting DSM-IV criteria for dementia. Depression illness was excluded by clinical interview and the Geriatric Depression Scale (GDS) of Yesavage (shorter form). The cutoff to be included in the study was 0-5. The diagnosis of MCI was finally based on a clinical consensus following evaluation in the Dementia Unit by a senior neurologist and a clinical neuropsychologist.

Inclusion criteria for the healthy elderly group were (i) no subjective memory complaints corroborated by neuropsychological exploration, (ii) CDR global score of 0 (no dementia), and (iii) normal independent function both judged clinically and by means of a standardized scale for the activities of daily living. None of them had a history of neurological, psychiatric disorders and/or major medical illness.

To avoid interference on EEG recordings and neuropsychological performance, the uptake of pharmacological compounds known to significantly affect any cognitive domain was considered cause of exclusion, both in healthy controls and MCI patients.

Individuals with medical conditions that may affect brain structure or function were also

excluded.

Apolipoprotein E genotyping

Genomic DNA was extracted from peripheral blood using short proteinase K digestion.

ApoE genotype was determined by PCR (polymerase chain reaction) amplification of the

polymorphic fragment of the ApoE gene, and digested by the restriction enzyme CfoI

using protocols previously described [Wenham et al., 1991].

Electroencephalographic recordings and pre-processing

Continuous EEG recordings were obtained in all participants in relaxed wakefulness with

eyes closed between 9-10 AM. Vigilance level was constantly controlled to avoid

intermittent alpha oscillatory behavior caused by the drowsiness state. EEG was

referenced to linked mastoids from 59 scalp locations (Fp1, Fp2, AF7, AF3, AFz, AF4,

AF8, F7, F5, F3, F1, Fz, F2, F4, F6, F8, FT7, FC5, FC3, FC1, FCz, FC2, FC4, FC6, FT8,

T7, C5, C3, C1, Cz, C2, C4, C6, T8, TP7, CP5, CP3, CP1, CPz, CP2, CP4, CP6, TP8, P7,

P5, P3, P1, Pz, P2, P4, P6, P8, PO7, PO3, POz, PO4, PO8, O1, and O2) according to the

International 10-20 system. Vertical and horizontal ocular movements were also

simultaneously recorded. Electrode-scalp impedance was always kept below 5 KΩ. All

electrophysiological variables were amplified (BrainAmp MR, Brain Vision®), filtered

(0.1-100 Hz bandpass), digitized (250 Hz, 16-bit resolution), and stored in digital format

for off-line analysis.

EEG epochs containing prominent ocular, muscular and/or any other type of artifacts were manually identified and eliminated. A total of 150 s of artifact-free EEG containing alpha rhythm were then available for each participant. The selected epochs were filtered within 6-13 Hz using a real and phase linear bandpass filter.

Determining the temporal dynamics of EEG-alpha sources

Synaptic flows of macroscopic activity between neuronal EEG sources (in our case EEG-alpha sources) were modeled using a multivariate autoregressive (MVAR) model [Astolfi et al., 2007, Astolfi et al., 2005; Supp et al., 2007]. This model implies that the time-varying neural current density responsible for the EEG scalp potentials is due to a set of K intracranial signal generators whose mutual dynamics $\mathbf{s}(t) = [s_1(t),...,s_K(t)]^T$ can be approximated by:

$$\mathbf{s}(t) = \sum_{\tau=1}^{p} \mathbf{B_s}(\tau)\mathbf{s}(t-\tau) + \mathbf{n}(t) \tag{1}$$

where p is the order of the MVAR model and $\mathbf{B}_s(\tau)$ is the K x K coefficient matrix corresponding to time-lag τ. The components of the multivariate residual process $\mathbf{n}(t) = [n_1(t),...,n_K(t)]^T$ are commonly assumed to be uncorrelated Gaussian processes.

We imposed two additional assumptions on this EEG model. Specifically, we assume that (1) the components of the residual process are not perfectly Gaussian and (2) the individual components of the multivariate residuals are mutually independent, i.e. they have zero second-order cross-correlations and zero higher-order dependencies. Conceptually, this is equivalent to assuming that the residuals of the model are the only

source of "new" or intrinsic information in each brain generator and that the MVAR

coefficient matrices are responsible for synaptic transfer between EEG sources. Indeed,

this approximation implicitely assumes that zero-lag neural flows of information are

negligible in comparison to time-lagged flows. This is plausible considering the presence

of axonal propagation delays [Freeman, 2000]. Within this framework, knowledge of

$\mathbf{B}_s(\tau)$ is sufficient to characterize the directionality of synaptic flow between brain

sources using e.g. the directed transfer function (DTF) [Kaminski et al., 2001].

A fundamental problem when studying functional relationships between brain areas is

that connectivity between scalp EEG signals is not equivalent to connectivity between

their underlying neural sources. This occurs because scalp EEG potentials do not

exclusively reveal averaged postsynaptic activity from localized cortical regions beneath

one electrode but the superposition of all active coherent neural sources located anywhere

in the brain, due to conduction in the head volume [Nunez and Srinivasan, 2006;

Hoechstetter et al., 2004]. Based on the quasi-static approximation of electrical

conduction in the head [Malmivuo and Plonsey, 1995] and using Eq. (1), we can assume

that the scalp EEG measurements, at M electrodes and at time instant t, denoted by $\mathbf{x}(t) =$

$[\mathbf{x}_1(t),\ldots,\mathbf{x}_M(t)]^T$, can be modeled as:

$$\mathbf{x}(t) = \mathbf{\Phi s}(t) = \sum_{\tau=1}^{p} \mathbf{\Phi B_s}(\tau)\mathbf{\Phi}^+\mathbf{x}(t-\tau) + \mathbf{\Phi n}(t) = \sum_{\tau=1}^{p} \mathbf{B_x}(\tau)\mathbf{x}(t-\tau) + \mathbf{v}(t) \qquad (2)$$

where $\mathbf{\Phi}$ is an M x K leadfield matrix containing the coefficients that project activity

from each brain source to the scalp electrodes and $^+$ denotes Moore-Penrose

pseudoinversion. Eq. (2) clearly shows that although the scalp EEG measurements are an

MVAR process, the corresponding MVAR coefficients are, in general, quite different from the MVAR coefficients driving the underlying brain sources, i.e. $\mathbf{B_x}(\tau) = \mathbf{\Phi}\mathbf{B_s}(\tau)\mathbf{\Phi}^+ \neq \mathbf{B_s}(\tau)$. Many previous studies have assumed exactly the opposite [Bernasconi and König, 1999; Baccalá and Sameshima, 2001; Kus et al., 2004], which makes their estimated functional connectivity diagrams questionable. Therefore, to obtain a valid characterization of the functional connectivity underlying EEG-alpha oscillations we need to estimate: (1) the MVAR coefficients driving the EEG-alpha sources, i.e. $\mathbf{B}_s(\tau)$ and (2) the leadfield matrix $\mathbf{\Phi}$. The former is needed to compute the DTF between EEG-alpha sources whereas the latter is required for estimating the intracranial location of the corresponding EEG-alpha generators.

To overcome volume conduction effects and to obtain the true underlying functional connectivity and the location of the brain areas involved in the generation of EEG alpha we used MVAR-EfICA, a novel non-invasive approach which has shown its superiority with respect to several other competing approaches [Gómez-Herrero et al., 2008]. A schematic representation of the analysis methology used in this study is shown in Figure 1, and consists of the following steps:

Principal component analysis (PCA)

PCA was applied to all healthy elderly subjects in order to reduce the effects of measurement noise and to remove second-order instantaneous cross-correlations caused by volume conduction [Richards, 2004]. Even more important, PCA reduces the dimensionality of the data and avoids ill-conditioned covariance matrices (from 59 EEG signals to just 5 principal components in most subjects) resulting in a faster and more

robust estimation of MVAR models. PCA linearly transforms the scalp EEG signals $\mathbf{x}(t)$ into a set of K mutually uncorrelated principal components (PCs). From Eq. (2) it follows that the PCA-transformed data is also an MVAR process with coefficients $\mathbf{B}_{PCA}(\tau)$ and multivariate residuals $\mathbf{r}(t)$:

$$\mathbf{x}_{PCA}(t) = \mathbf{C}\mathbf{x}(t) = \sum_{\tau=1}^{p} \mathbf{C}\mathbf{\Phi}\mathbf{B}_{s}(\tau)(\mathbf{C}\mathbf{\Phi})^{-1}\mathbf{x}_{PCA}(t-\tau) + \mathbf{C}\mathbf{\Phi}\mathbf{n}(t) = \sum_{\tau=1}^{p} \mathbf{B}_{PCA}(\tau)\mathbf{x}_{PCA}(t-\tau) + \mathbf{r}(t) \qquad (3)$$

where $\mathbf{C}$ is a K x M matrix implementing the PCA transformation. We used as many PCs as necessary to reconstruct most (99%) of the variance explained by the original EEG signals.

Multivariate Autoregressive (MVAR) modeling

In all healthy elderly subjects, an MVAR model was fitted to the PCs obtained in the previous step using the algorithm ARfit [Schneider and Neumaier, 2001]. $\hat{\mathbf{B}}_{PCA}(\tau) \approx \mathbf{B}_{PCA}(\tau)$ denotes the estimated model coefficients and $\hat{\mathbf{r}}(t) \approx \mathbf{r}(t)$ denotes the estimated model residuals. The model order was 7 in all cases and was automatically selected using Swartz's Bayesian Criterion (SBC) [Schwarz, 1978]. Namely, we picked the order that guaranteed that greater model orders did not significantly reduce the SBC, i.e. the order for which the reduction in the SBC had reached 90% of the maximum reduction achievable within the tested range of model orders (model orders tested in the present study ranged from 2 to 30). This modified SBC criterion was motivated by the fact that, for our EEG datasets, both SBC and Akaike's information criterion dropped

monotonically as the model order increased, which is in close correspondence with

previous EEG studies [Supp et al., 2007; Brovelli et al., 2004].

Independent component analysis (ICA)

As mentioned above, we assumed that the components of the multivariate residual

process driving the EEG-alpha sources in Eq. (1) (denoted by $\mathbf{n}(t)$) are mutually

independent. Moreover, Eq. (3) shows that the residual process found in the previous step

($\mathbf{r}(t) = (\mathbf{C\Phi})\mathbf{n}(t)$ in Eq. (3)) is just a linear mixture of the components of $\mathbf{n}(t)$. Therefore,

we applied ICA [Koldovsky et al., 2006] to invert that mixing by estimating a K x K

matrix $\hat{\mathbf{W}} \approx (\mathbf{C\Phi})^{-1}$ that minimized the mutual dependencies between the components of

the multivariate residual process $\mathbf{r}(t)$. Then, from the relationship $\hat{\mathbf{W}} \approx (\mathbf{C\Phi})^{-1}$ we can

easily obtain an estimate of the leadfield matrix: $\hat{\mathbf{\Phi}} = (\hat{\mathbf{W}}\mathbf{C})^{+} \approx \mathbf{\Phi}$. Finally, the activation

patterns of the underlying EEG-alpha sources were obtained by spatially filtering the

scalp EEG measurements: $\hat{\mathbf{s}}(t) = \hat{\mathbf{\Phi}}^{+}\mathbf{x}(t) = \hat{\mathbf{\Phi}}^{+}\mathbf{\Phi}\mathbf{s}(t) \approx \mathbf{s}(t)$. Each of the K rows of matrix

$\hat{\mathbf{\Phi}}^{+}$ is a spatial filter retrieving an individual EEG-alpha source. In the following we will

show $\hat{\mathbf{F}} = \hat{\mathbf{\Phi}}^{+}$. Due to the scale indeterminacy inherent to ICA methods, only the

waveform (but not the scale) of the EEG-alpha sources can be recovered. That is, the

norm of the columns of the estimated leadfield matrix is arbitrary. Note, however, that

this scale indeterminacy is irrelevant for either localizing the EEG sources or computing

their mutual directional interactions.

Assessing the significance of ICA estimates

Most ICA algorithms and specifically EfICA [Koldovsky et al., 2006] involve stochastic optimization, which raises concerns regarding reliability when applying them to real data [Särelä and Vigario, 2003]. To overcome this issue, we identified clusters of ICA estimates (EEG-alpha sources) that were consistently found across random initializations of the ICA algorithm, across random bootstrap surrogates of the input data [Himberg et al., 2004], and (across) healthy elderly subjects [Gómez-Herrero et al., 2008]. The validity of the clustering results was assessed using the R-index [Himberg et al., 2004]. Each cluster was uniquely represented by a single centrotype EEG-alpha source. The centrotype was defined as the ICA-estimate showing the maximum sum of similarities to other points in one cluster. The similarity between two ICA estimates was assessed using the cross-correlation coefficient between their spatial distribution of scalp potentials. Only centrotypes of significant clusters were considered as valid EEG-alpha sources. A cluster was considered as significant if it contained ICA-estimates from at least 70% of the analyzed healthy elderly subjects (high inter-subject repeatability) and from at least 90% of the ICA-runs corresponding to those subjects (high intra-subject reliability). Each centrotype EEG-alpha source was characterized by two spatial features: (1) the spatial filter (a row vector of M coefficients $\mathbf{f}_i=[f_{i,1},\ldots, f_{i,M}]$) retrieving the temporal activation of the EEG-alpha source from the scalp EEG measurements, i.e. the corresponding row of the pseudoinverse of the leadfield matrix ($\hat{\mathbf{\Phi}}^{+}$) associated with the centrotype ICA estimate, and (2) the scalp distribution of potentials (a column vector of M coefficients $\mathbf{g}_i=[g_{i,1},\ldots, g_{i,M}]^{T}$) generated by the centrotype EEG-alpha source, i.e. the corresponding column of the leadfield matrix $\hat{\mathbf{\Phi}}$ associated with the centrotype ICA estimate. Figure 2 shows the analysis steps followed to assess the significance of ICA estimates used to

determine both the intracranial location of EEG-alpha sources and the directionality of synaptic flow between them.

The features of the K centrotype EEG-alpha sources underlying the healthy elderly population was therefore summarized by a single leadfield matrix $\hat{\mathbf{\Phi}}_{control} = [\mathbf{g}_1,...,\mathbf{g}_K]$ and a single set of spatial filters $\hat{\mathbf{F}}_{control} = [\mathbf{f}_1^T,...,\mathbf{f}_K^T]^T$.

Determining the intracranial location of EEG-alpha centrotypes

We used the global leadfield matrix obtained for the healthy elderly population ($\hat{\mathbf{\Phi}}_{control}$) to determine the intracranial locations of the EEG-alpha centrotypes. Each column of $\hat{\mathbf{\Phi}}_{control}$ defines the distribution of scalp potentials generated by each individual EEG-alpha source. The brain locations corresponding to these potentials were obtained using a 3D brain space. The activation probability of each grid element in this brain space was computed by the standardized weighted low-resolution brain electromagnetic tomography (swLORETA) [Palmero-Soler et al., 2007]. A realistic head model of three layers (scalp, skull and brain with conductivities of 0.33, 0.0042, and 0.33, respectively) was used for this purpose. Although previous studies have shown that inter-subject variability in the electric resistivities of these layers may affect the error sources in EEG modeling [Gonçalves et al., 2003; Oostendorp et al., 2000], we did not have the possibility of measuring them *in vivo* for each participant in the present study. Source reconstruction solutions were projected onto the 3D MR images of the Collin's brain provided by the Montreal Neurological Institute. Probabilities of source activation based on Fisher's F-test were obtained for two subdivisions of the alpha band (lower alpha: 7.5-10 Hz; upper

alpha: 10.1-12.5 Hz) for each independent alpha-EEG source, both in healthy elderly subjects and MCI patients. This subdivision of the alpha band was performed considering previous evidence that highlighted the differential effects of normal aging and mild dementia on different portions of the classic alpha band [Moretti et al., 2004].

Computing directional connectivity between EEG-alpha sources

The obtained centrotype spatial filters $\hat{\mathbf{F}}_{control} = \left[\mathbf{f}_1^T, ..., \mathbf{f}_K^T\right]^T$ were employed to determine the temporal activation patterns of each EEG-alpha source in individual subjects (both in controls and MCI). For an arbitrary subject (control or MCI) the activation of the ith centrotype was obtained as $\mathbf{s}_i(t) = \mathbf{f}_i \mathbf{x}(t)$, where $\mathbf{x}(t)$ is a column vector with the scalp EEG measurements of that subject at time instant t. Subsequently, an MVAR model was fitted to these centrotype activations using the same estimation algorithm and model order selection method as described above. Then, the normalized DTF [Kaminski et al., 2001] was applied to determine directional causal relationships between these temporal activation patterns. Normalized values of the DTF from the jth to the ith EEG-alpha source at a certain frequency f ranged from 0 to 1. Values close to 1 indicated that the neural dynamics of the source *i* are mostly explained by a directed flow of synaptic activity from the source *j*. DTF values close to 0 denoted that there was no significant synaptic flow from source *j* to source *i* at that EEG frequency. The DTF between EEG-alpha sources was computed for both healthy elderly subjects and MCI patients.

Computing the alpha peak frequency

The alpha peak frequency was computed for the temporal activation of each EEG-alpha source. Spectral power was estimated using the Welch's averaged modified periodogram (4 s segments, 1 Hz resolution, 50% overlapping, and Hanning windowing) as implemented in MATLAB$^®$ v. 7.4 (The MathWorks, Inc.). Alpha peak frequency was identified as the maximum spectral power value within the defined alpha band (7.5-12.5 Hz).

Statistical analysis

In order to assess the statistical significance of the normalized DTF values obtained, the surrogates-based procedure proposed by [Theiler et al., 1992] was used. DTF values below the confidence threshold ($p < 0.01$) were considered not significant and removed from the analysis.

Alpha peak frequency, probability of source activation and directionality of the synaptic flow were evaluated with two types of mixed ANOVAs: i) without including covariates; and ii) with scores provided by the Mini Mental State Examination (MMSE) and age as covariates (if they were significant, otherwise this ANOVA was not performed). Each covariate was tested independently for significance, and only significant covariates ($p < 0.05$) were included in the final ANOVA. Mauchly's *W* was computed to check for violations of the sphericity assumption. When Mauchly's *W* test was significant, the Greenhouse–Geisser correction was applied to all repeated-measures analyses (original degrees of freedom and the corresponding epsilon value were reported; p value reflects the epsilon correction). Homogeneity of variance was evaluated with Levene's test. The

Student-Newman-Keuls or the Games-Howell procedures were applied for multiple post hoc comparisons depending on population variances.

In order to confirm previous reports of alpha slowing in MCI patients, alpha peak frequency was evaluated with a mixed ANOVA including, as the within-subject factor, the electrodes showing the maximum amplitude within the alpha band for each EEG-alpha centrotype as determined by the MVAR-EfICA procedure, and group (healthy elderly and MCI) as the between-subject factor.

Activation probabilities of different EEG-alpha sources were analyzed for the lower and upper alpha band separately in controls and MCI patients. The ANOVA included EEG-alpha source (see below the three different sources that achieved statistical significance) as the within-subject factor and group (healthy elderly and MCI) as the between-subject factor. A similar statistical design was applied to evaluate the directionality of the synaptic flow between EEG-alpha sources.

In the present study, a higher number of MCI patients showed the allele ε4 in the ApoE (p < 0.04) when compared to healthy elderly subjects. As the presence of this allele has been associated with an increased risk of conversion to AD [Caselli et al., 2007; Wang et al., 2002; Corder et al., 1993], a new set of mixed ANOVAs was performed in MCI patients to evaluate its effect on each dependent variable separately. In this particular case, genotype (presence or absence of ε4) instead of group was introduced in the different ANOVAs as the between-subject factor.

Results

Spatial patterns of EEG-alpha rhythm

The R-index statistic indicated that 10 clusters described best the observed data among all the possible partitions obtained by the hierarchical clustering algorithm. Out of those 10 clusters, only three (clusters 7, 9 and 10) satisfied the established statistical criteria for being considered EEG-alpha sources (Figure 2). First, clusters 7, 9 and 10 were by far the largest with 1125, 1050 and 1050 ICA-estimates, respectively. Second, they contained estimates from 75%, 70%, and 70% of the healthy elderly subjects, respectively, indicating a high inter-subject repeatability.

Intracranial location of EEG-alpha centrotypes

Coordinates of the Talairach-Tournoux atlas were employed to determine the anatomical location of the single electric dipole best explaining the scalp distribution of each centrotype ICA-estimate for the three significant clusters mentioned above. The electric dipole corresponding to cluster 7 was located in caudal regions of the thalamus (x=9, y=-25, z=9), cluster 9 showed its maximum activation in the precuneus (x=2, y=-60, z=28) and cluster 10 was located in the middle occipital gyrus, within the limits of the cuneus (x=11, y=-97, z=13). Figure 3 displays the brain sources of the alpha rhythm based on the selected cluster.

Alpha peak frequency in healthy aging and MCI

The alpha peak frequency corresponding to the thalamic, precuneus and cuneus EEG-alpha sources was obtained for controls and MCI patients. As there were no significant

main effects of the MMSE scores and age on the alpha peak frequency, these two covariates were not included in the ANOVA. As expected, MCI patients showed a significant decrease in the alpha peak frequency as compared to controls [$F(1,38) = 7.02$; $p < 0.02$]. On the average, the alpha peak frequency in MCI patients was 0.6 Hz (SE = 0.17) lower than in controls. This abnormal slowing was evident for the three EEG-alpha sources (see Table 2), independent of the presence of the allele ε4.

EEG-alpha source activation in healthy aging and MCI

Figure 4 shows source activation probabilities of the lower and upper alpha subdivisions in controls and MCI patients for each EEG-alpha source.

As for the alpha peak frequency, no covariates (MMSE and age) were included in the variance model. The ANOVA showed a significant effect of the EEG-alpha source in the lower alpha band [$F(2,76) = 19.89$; $p = 0.005$]. Specifically, this activation probability was lower in precuneus than in thalamus ($p < 0.001$) or cuneus ($p < 0.04$). The ANOVA also revealed that MCI patients showed a significantly higher activation (~19%) during lower alpha generation as compared to controls [$F(1,38) = 5.84$; $p < 0.03$], but this abnormal enhancement was only significant for the thalamic source [$F(1,38) = 9.09$; $p < 0.005$] (see Figure 4, top panel). No differences were found between healthy elderly subjects and MCI patients for the upper alpha band.

The two-way ANOVAs (EEG-alpha source × genotype) conducted in MCI patients for the lower and upper alpha band showed neither a main effect of genotype nor interaction effect.

Directional connectivity between EEG-alpha sources

The two-way ANOVA (with MMSE as covariate) performed to evaluate the directionality of the synaptic flow between thalamus, cuneus and precuneus within the lower alpha band showed a significant group effect and a significant directionality x group interaction ($p < 0.04$). In agreement with the enhanced activation of the thalamic alpha source observed in the MCI group, the synaptic transfer was also abnormally facilitated in these patients (~24% higher) relative to controls, particularly from thalamus to cortex (~38% higher in MCI; $p < 0.008$). This effect was similar in MCI ε4-carriers and non-carriers. No differences between controls and MCI patients were obtained for cortico-cortical interactions in the lower alpha band. Analyses only revealed a higher flow of synaptic activity from cuneus to precuneus than in the opposite direction [$F(1,38) = 22.61$; $p < 0.00003$]. Figure 5 shows comparisons of DTF values obtained between brain sources participating in the generation of lower alpha oscillations.

For the upper alpha subdivision, the three-way ANOVA (with age as covariate) revealed a significant group effect [$F(1,37) = 9,32$; $p < 0.005$]. In particular, MCI patients showed a decreased bidirectional synaptic flow of about 32% between thalamic and cortical sources when compared to healthy elderly subjects. Analyses also showed a significant interaction between the factors group and age [$F(2,37) = 8.17$; $p < 0.002$]. In agreement with this finding, we found that the bidirectional synaptic flow between thalamocortical sources of the upper alpha band significantly decreased with age in healthy elderly subjects but not in MCI patients. The scatter plot shown in Figure 6 depicts the degree of linear relationship between these two factors in both groups as derived from Pearson's correlation. As shown, regression fitness reached statistical significance only for healthy

elderly subjects (p < 0.01) suggesting that the strength of the thalamocortical synaptic

flow within the upper alpha decreases with age as a result of normal aging processes. No

significant effects were found for cortico-cortical interactions in the upper alpha band in

any of the groups.

Like the remaining dependent variables, no differences between controls and MCI were

found when the influence of genotype on directional connectivity was compared in both

subdivisions of the alpha band.

Discussion

In the present study, we have examined whether alterations in the directionality of the

synaptic flow between EEG-alpha sources were able to distinguish amnesic MCI patients

from cognitively intact elderly individuals. In addition to the typical EEG-alpha slowing

associated with neurodegenerative disorders, MCI patients also showed an abnormal

enhancement of the thalamic source activation together with a facilitation of synaptic

transmission from thalamus to cortex restricted to the lower alpha range (7.5-10 Hz).

These findings reveal, for the first time, that thalamic dysfunctions account for

abnormalities of the alpha rhythm in MCI patients, thereby providing new insights into

the role of thalamocortical integrity in the preclinical stages of AD.

Thalamocortical generation of alpha oscillations in healthy aging

Animal studies have shown that much of the patterning of the alpha rhythm is subject to

controlling influence from synchronizing pacemakers within thalamocortical networks

[Lopes da Silva, 1991; Steriade et al., 1990a]. Our results provide additional support for

this hypothesis in humans. We found that thalamus together with the cuneus and precuneus were the main generators of alpha oscillations under resting EEG conditions. This finding is in agreement with results obtained by Schreckenberger and colleagues [Schreckenberger et al., 2004] who reported a positive correlation between EEG alpha power and metabolism of the lateral thalamus as well as occipital cortex (cuneus) and adjacent parts of the parietal cortex (precuneus) in humans.

The main obstacle to estimate the sources of electrical activity in the thalamus comes from the spatial arrangement of neurons in thalamic nuclei resulting in a closed field [Lopes da Silva and Van Rotterdam, 1993]. Indeed, the three-dimensional symmetry of the dendritic organization in thalamic neurons makes it difficult to determine distant neuronal contributions to scalp-recorded electric potentials [Druckman and Lacey, 1989]. In contrast, previous studies have determined unambiguous thalamic sources of scalp EEG phenomena [Gobbelé et al., 2004; Trujillo-Barreto et al., 2004; Isaichev et al., 2001] suggesting that thalamic oscillations can be captured under specific experimental manipulations. Further evidence has shown that the highest degree of cross-correlation in the alpha range between the lateral pulvinar nucleus and different cortical regions was observed in the precentral area (Fujita et al., 1979) where the electrode that best represented the thalamic centrotype was located in the present study.

Our results also revealed that thalamocortical synaptic transmission remained alike from thalamus to cortex and vice versa. These findings, together with results from human studies employing 3D equivalent dipole modeling [Isaichev et al., 2001; Başar et al., 1997; Pritchard and Duke, 1997; Schurmann et al., 2000], support the notion that complex interactions between local and non-local EEG sources, instead of a single or

multiple isolated neural generators, are responsible for the genesis of the human alpha

rhythm in normal aging [Nunez et al., 2001].

Thalamic dysfunction at generating alpha oscillations in MCI

Alpha slowing together with the enhanced activation of the thalamic source for the lower

alpha band indicates a dysfunctional state of this subcortical structure in MCI patients.

The alpha slowing has been consistently reported in EEG studies of AD [e.g., Moretti et

al., 2004], but results are contradictory in MCI patients. To date, only one study has

shown that the mean frequency peak of alpha rhythm was significantly lower in MCI

when compared to healthy elderly subjects, and significantly higher when compared to

AD patients [Fernandez et al., 2006]. Other studies, however, either found no differences

between MCI and controls [Huang et al., 2000; Jelic et al., 1996], or only showed a slight

tendency toward a reduction of the alpha peak frequency [Osipova et al., 2006].

A chronically slowed alpha rhythm during resting wakefulness has been suggested as a

definitive indicator of underlying neurological pathology [Niedermeyer, 1997], but

mechanisms by which alpha oscillations slow down have not yet been revealed in

humans. Evidence from *in vitro* preparations of the cat lateral geniculate nucleus has

shown that a moderate activation of metabotropic glutamate receptors can lead to a

deceleration of alpha waves through a slowing of high-threshold bursting neurons

interconnected by gap junctions [Hughes et al., 2004]. Should this cellular mechanism be

affected to some extent by the pathogenesis of AD, the EEG-alpha rhythm would also be

affected. In support of this hypothesis, amyloid deposits are not only present in the

neocortex but also in deep gray matter structures as the thalamus [Rudelli et al., 1984;

Masliah et al., 1989; Braak and Braak, 1991]. Evidence further suggests that β-amyloid plaques may disrupt the glutamatergic system by affecting simultaneously different signaling pathways [reviewed by Parameshwaran et al., 2008]. Should this also be the case in MCI, inhibition of glutamate receptors might account for the slowing of alpha oscillations and for the abnormal enhanced synchrony between in-phase and anti-phase groups of high-threshold bursting neurons of the thalamus [for a description of electrophysiological properties of the thalamocortical neurons see Hughes and Crunelli, 2007].

Other authors [e.g., Llinás et al., 1999] have reported a shift from a normal alpha rhythm to a robust low-frequency theta across a diverse selection of neurological and psychiatric disorders, which strongly correlated with the presence of positive symptoms. Based on these results, it could be postulated that the thalamic dysfunction at generating alpha oscillations might not be specific to AD. However, we would like to bring to the attention of the reader two important factors that could have influenced the results reported by Llinás and colleagues. First, controls and patients were not of the same age (controls ranged between 24 and 45 yrs; patients ranged between 28 and 73 yrs) which might be an important issue of confusion in this study because alpha oscillations become slower with age. And second, results were based on averaging cerebral oscillations of four patients diagnosed with Parkinson's disease, one patient with tinnitus, two patients with neurogenic pain, and two patients with major depression. The latter approach impeded statistical confirmation of the decrease of alpha and increase of theta in each patient population. Although the present study could not determine whether alpha slowing is specific to AD, it describes for the first time specific abnormalities underlying alpha

generation in a high-risk population for the development of AD. It remains to ascertain whether or not the enhanced facilitation of thalamic and thalamocortical synaptic transmission is common to abnormal alpha generation in other neurological and neuropsychiatric disorders.

Thalamocortical dysfunctions at generating alpha oscillations in MCI

Animal studies have shown that the posterior parietal gyri and the occipital lobes receive major inputs from caudal portions of the thalamus, including pulvinar and the lateral geniculate nucleus [Steriade et al., 1997]. Changes in the behavior of large ensembles of thalamocortical relay cells or alterations in this complex circuitry are reflected in the cortical EEG oscillations [Steriade et al., 1990b], providing an *in vivo* global measurement of thalamocortical integrity in a variety of cerebral diseases. In agreement with this idea, MCI patients showed abnormal synaptic transmission between thalamus and cortex in generating alpha oscillations. In particular, synaptic flow from thalamus to cortex was facilitated for the lower alpha band in MCI relative to healthy elderly subjects; whereas for the upper alpha band, transmission between thalamus and cortex decreased in both directions. These changes in thalamocortical functional connectivity may reveal modifications in intrinsic membrane properties of the thalamic neurons or synaptic dysfunctions between excitatory and inhibitory neuronal populations involved in the generation of rhythmic EEG activity. Whereas a progressive decrease of thalamocortical transmission in the upper alpha band is expected with increasing normal aging (see Figure 6), the parallel gradual increase of thalamocortical synchrony in the lower alpha might signal the route to functional decline in MCI, these patients becoming more

vulnerable for the development of AD. Future longitudinal studies in MCI patients who will later convert to AD are necessary to confirm this hypothesis.

White matter damage [e.g., Duan et al., 2006; Bozzali et al., 2002] and aberrant patterns of functional connectivity [e.g., Wang et al., 2007; Rombouts et al., 2005; Greicius et al., 2004] between different brain regions have been suggested as accounting for the cognitive deficits observed in AD patients. Thus, studies using resting-state functional magnetic resonance imaging (fMRI) have shown that abnormal functional connectivity patterns in AD not only include decreased correlations between anterior and posterior regions of the brain but also increased positive correlations within the prefrontal lobe, parietal lobe and occipital lobe [Wang et al. 2007]. Consistent with these results, it has been found that MCI patients show less deactivation of the default mode network (involving anterior frontal, precuneus and posterior cingulate cortex) as compared to healthy elderly subjects, but more deactivation when compared to AD patients [Rombouts et al. 2005]. Taken together, metabolic and electrophysiological results indicate that abnormal enhancement of functional connectivity could be used as surrogate markers at improving the ability to differentiate patients with high risk of AD from healthy elderly subjects.

Relationship between ApoE4 and thalamocortical dysfunction in MCI

Gene dosage of the ApoE ε4 allele is a major risk factor for familial AD of late onset [Corder et al., 1993]. But the interaction between this genotype and the integrity of thalamocortical circuits involved in alpha generation has not been explored to date in either healthy aging or MCI patients. The present study showed that a significantly higher

number of MCI patients had the allele ε4 in the ApoE when compared to controls, confirming previous findings that the presence of the ε4 allele is more frequent in persons with MCI than in healthy elderly [Caselli et al., 2007; Wang et al., 2002]. However, no relationship was found between directional changes of thalamocortical synaptic flow during alpha generation and the presence of the ε4 allele in the present study. Despite the increased risk of ε4 carriers to develop AD, MCI population also contains ε4 carriers who may or may not develop a neurodegenerative condition. The intrinsic heterogeneity of this group and the small size of our sample population may account for the absence of significant relationships between changes in brain mechanisms of alpha generation and the presence of the ε4 allele in our MCI sample. Alternatively, it might happen that thalamic facilitation within the lower-alpha band was not specific to MCI but a more global marker of neurological/psychiatric dysfunction, accounting for the lack of correlation with the APOE ε4 genotype that seems to be more specific to AD disease. Finally, it could be further hypothesized that once changes in thalamocortical dynamics underlying EEG-alpha slowing appear, the carrier status of apoe4 could no longer be relevant. Experimental support for this hypothesis comes from large-community based studies that did not find a significant influence of the APOE ε4 on the rate of AD progression in cognitive or functional domains [Kleiman et al., 2006; Hoyt et al., 2005].

In summary, results from the present study suggest that abnormal functioning of thalamocortical networks accounts for differences in EEG-alpha slowing between MCI patients and healthy elderly subjects. Future follow-up studies will confirm whether or not these changes parallel cognitive decline, thereby providing a reliable *in vivo* functional marker to predict which patients diagnosed with MCI will convert to AD.

References

Astolfi L, Bakardjian H, Cincotti F, Mattia D, Marciani MG, De Vico Fallan F, Colosito A, Salinari S, Miwakeichi F, Yamaguchi Y, Martinez P, Cichocki A, Tocci A, Babiloni F (2007): Estimate of causality between independent cortical spatial patterns during movement volition in spinal cord injured patients. Brain Topogr 19:107-123.

Astolfi L, Cincotti F, Mattia D, Babiloni C, Carducci F, Basilisco A, Rossini PM, Salinari S, Ding L, Ni Y, He B, Babiloni F (2005): Assessing cortical functional connectivity by linear inverse estimation and directed transfer function: simulations and application to real data. Clin Neurophysiol 116:920-932.

Babiloni C, Binetti G, Cassetta E, Dal Forno G, Del Percio C, Ferreri F, Ferri R, Frisoni G, Hirata K, Lanuzza B, Miniussi C, Moretti DV, Nobili F, Rodriguez G, Romani GL, Salinari S, Rossini PM (2006): Sources of cortical rhythms change as a function of cognitive impairment in pathological aging: a multicenter study. Clin Neurophysiol 117:252-268.

Babiloni C, Miniussi C, Babiloni F, Carducci F, Cincotti F, Del Percio C, Sirello G, Fracassi C, Nobre AC, Rossini PM (2004): Sub-second "temporal attention" modulates alpha rhythms. A high-resolution EEG study. Cogn Brain Res 19:259-268.

Baccalá LA and Sameshima K (2001): Partial directed coherence: A new concept in neural structure determination. Biol Cybern 84:463-474.

Basar E, Schürmann M, Basar-Eroglu C, Karakaş S (1997): Alpha oscillations in brain functioning: an integrative theory. Int J Psychophysiol 26:5-29.

Bernasconi C and König P (1999): On the directionality of cortical interactions studied by structural analysis of electrophysiological recordings. Biol Cybern 81:199-210.

Bozzali M, Falini A, Franceschi M, Cercignani M, Zuffi M, Scotti G, Comi G, Filippi M (2002): White matter damage in Alzheimer's disease assessed in vivo using diffusion tensor magnetic resonance imaging. J Neurol Neurosurg Psychiatry 72:742-746. Links

Braak H and Braak E (1991): Demonstration of amyloid deposits and neurofibrillary changes in whole brain sections. Brain Pathol 1:213-216.

Brovelli A, Ding M, Ledberg A, Chen, Y, Nakamura R, Bressler S (2004). Beta oscillations in a large-scale sensorimotor cortical network: Directional influences revealed by granger causality. Proc Natl Acad Sci USA 101:9849-9854.

Caselli RJ, Reiman EM, Locke DE, Hutton ML, Hentz JG, Hoffman-Snyder C, Woodruff BK, Alexander GE, Osborne D (2007): Cognitive domain decline in healthy apolipoprotein E epsilon4 homozygotes before the diagnosis of mild cognitive impairment. Arch Neurol 64:1306-1311.

Corder EH, Saunders AM, Strittmatter WJ, Schmechel DE, Gaskell PC, Small GW, Roses AD, Haines JL, Pericak-Vance MA (1993): Gene dose of apolipoprotein E type 4 allele and the risk of Alzheimer's disease in late onset families. Science 261:921-923.

De Jong LW, van der Hiele K, Veer IM, Houwing JJ, Westendorp RG, Bollen EL, de Bruin PW, Middelkoop HA, van Buchem MA, van der Grond J (2008). Strongly reduced volumes of putamen and thalamus in Alzheimer's disease: an MRI study. Brain 131:3277-3285.

De Munck JC, Gonçalves SI, Huijboom L, Kuijer JP, Pouwels PJ, Heethaar RM, Lopes da Silva FH (2007): The hemodynamic response of the alpha rhythm: An EEG/fMRI study. Neuroimage 35:1142-1151.

De Rover M, Petersson KM, van der Werf SP, Cools AR, Berger HJ, Fernandez G (2008): Neural correlates of strategic memory retrieval: differentiating between spatial-associative and temporal-associative strategies. Hum Brain Mapp 29:1068-1079.

Druckman D, Lacey JI. 1989. Brain and cognition. Some new technologies. Washington: National Academy Press.

Duan JH, Wang HQ, Xu J, Lin X, Chen SQ, Kang Z, Yao ZB (2006): White matter damage of patients with Alzheimer's disease correlated with the decreased cognitive function. Surg Radiol Anat 28:150-156.

Fernandez A, Hornero R, Mayo A, Poza J, Gil-Gregorio P, Ortiz T (2006): MEG spectral profile in Alzheimer's disease and mild cognitive impairment. Clin Neurophysiol 117:306-314.

Freeman WJ (2000): Characteristics of the synchronization of brain activity imposed by finite conduction velocities of axons. Int J Bifurcation Chaos 10:2307-2322.

Fujita S, Fujita K, Matsumoto S (1979): Cross-correlation analysis of the lateral pulvinar and scalp EEG in man. Appl Neurophysiol 42:294-301.

Gobbele R, Waberski TD, Simon H, Peters E, Klostermann F, Curio G, Buchner H (2004): Different origins of low- and high-frequency components (600 Hz) of human somatosensory evoked potentials. Clin Neurophysiol 115:927-937.

Gómez-Herrero G, Atienza M, Egiazarian K, Cantero JL (2008): Measuring directional coupling between EEG sources. Neuroimage 43:497-508.

Gonçalves S, de Munck JC, Verbunt JPA, Heethaar RM, Lopes da Silva FH (2003): *In vivo* measurement of the brain and skull resistivities. Using an EIT-based method and the combined analysis of SEF/SEP data. IEEE T Biomed Eng 50:1124-1128.

Greicius MD, Srivastava G, Reiss AL, Menon V (2004): Default-mode network activity distinguishes Alzheimer's disease from healthy aging: evidence from functional MRI. Proc Natl Acad Sci USA 101:4637-4642.

Guillozet AL, Weintraub S, Mash DC, Mesulam MM (2003): Neurofibrillary tangles, amyloid, and memory in aging and mild cognitive impairment. Arch Neurol 60:729-736.

Himberg J, Hyvärinen A, Esposito F (2004): Validating the independent components of neuroimaging time-series via clustering and visualization. Neuroimage 22:1214-1222.

Hoechstetter K, Bornfleth H, Weckesser D, Ille N, Berg P, Scherg M (2004): BESA source coherence: A new method to study cortical oscillatory coupling. Brain Topogr 16:233-238.

Hoyt BD, Massman PJ, Schatschneider C, Cooke N, Doody RS (2005): Individual growth curve analysis of APOE epsilon 4-associated cognitive decline in Alzheimer disease. Arch Neurol 62:454-459.

Huang C, Wahlund L, Dierks T, Julin P, Winblad B, Jelic V (2000): Discrimination of Alzheimer's disease and mild cognitive impairment by equivalent EEG sources: a cross-sectional and longitudinal study. Clin Neurophysiol 11:1961-1967.

Hughes SW, Lörincz M, Cope DW, Blethyn KL, Kekesi KA, Parri HR, Juhasz G, Crunelli V (2004): Synchronized oscillations at alpha and theta frequencies in the lateral geniculate nucleus. Neuron 42:253-268.

Hughes SW and Crunelli V (2005): Thalamic mechanisms of EEG alpha rhythms and their pathological implications. Neuroscientist 11:357-372.

Hughes SW, Crunelli V (2007): Just a phase they're going through: the complex interaction of intrinsic high-threshold bursting and gap junctions in the generation of thalamic alpha and theta rhythms. Int J Psychophysiol 64:3-17.

Isaichev SA, Derevyankin VT, Koptelov YM, Sokolov EN (2001): Rhythmic alpha-activity generators in the human EEG. Neurosci Behav Physiol 31:49-53.

Jelic V, Shigeta M, Julin P, Almkvist O, Winblad B, Wahlund LO (1996): Quantitative electroencephalography power and coherence in Alzheimer's disease and mild cognitive impairment. Dementia 7:314-323.

Kaminski M, Ding M, Truccolo WA, Bressler S (2001): Evaluating causal relations in neural systems: Granger causality, directed transfer function and statistical assessment of significance. Biol Cybern 85:145-157.

Karas GB, Scheltens P, Rombouts SA, Visser PJ, van Schijndel RA, Fox NC, Barkhof F (2004): Global and local gray matter loss in mild cognitive impairment and Alzheimer's disease. Neuroimage 23:708-716.

Kleiman T, Zdanys K, Black B, Rightmer T, Grey M, Garman K, Macavoy M, Gelernter J, van Dyck C (2006): Apolipoprotein E epsilon4 allele is unrelated to cognitive or functional decline in Alzheimer's disease: retrospective and prospective analysis. Dement Geriatr Cogn Disord 22:73-82.

Koldovský Z, Tichavský P, Oja E (2006): Efficient variant of algorithm fastica for independent component analysis attaining the Cramer-Rao lower bound. IEEE T Neural Networks 17:1265-1277.

Kús R, Kaminski M, Blinowska K (2004): Determination of EEG activity propagation: pair-wise versus multichannel estimate. IEEE T Biomed Eng 51:1501-1510.

Lopes da Silva F (1991): Neural mechanisms underlying brain waves: from neural membranes to networks. Electroencephalogr Clin Neurophysiol 79:81-93.

Lopes da Silva F and Van Rotterdam A (1993): Biophysical aspects of EEG and magnetoencephalogram generation. In: Niedermeyer E and Lopes da Silva FH, editor. Electroencephalography. Basic principles, clinical applications and related fields. Baltimore: Williams and Wilkins. p 78-91.

Llinás RR, Ribary U, Jeanmonod D, Kronberg E, Mitra PP (1999): Thalamocortical dysrhythmia: A neurological and neuropsychiatric syndrome characterized by magnetoencephalography. Proc Natl Acad Sci USA 96:15222-15227.

Llinás R, Urbano FJ, Leznik E, Ramírez RR, van Marle HJ (2005): Rhythmic and dysrhythmic thalamocortical dynamics: GABA systems and the edge effect. Trends Neurosci 28:325-333.

Malmivuo J, Plonsey R. 1995. Bioelectromagnetism: Principles and applications of bioelectric and biomagnetic fields. New York: Oxford University Press.

Markesbery WR, Schmitt FA, Kryscio RJ, Davis DG, Smith CD, Wekstein DR (2006): Neuropathologic substrate of mild cognitive impairment. Arch Neurol 63:38-46.

Masliah E, Terry R, Buzsaki G (1989): Thalamic nuclei in Alzheimer disease: evidence against the cholinergic hypothesis of plaque formation. Brain Res 493:241-246.

McCormick DA (1999): Are thalamocortical rhythms the rosseta stone of a subset of neurological disorders? Nature Med 5:1349-1351.

Moretti DV, Babiloni C, Binetti G, Cassetta E, Dal Forno G, Ferreric F, Ferri R, Lanuzza B, Miniussi C, Nobili F, Rodriguez G, Salinari S, Rossini PM (2004): Individual analysis of EEG frequency and band power in mild Alzheimer's disease. Clin Neurophysiol 115:299-308.

Morrison JH and Hof PR (1997): Life and death of neurons in the aging brain. Science 278: 412-419.

Niedermeyer E (1997): Alpha rhythms as physiological and abnormal phenomena. Int J Psychophysiol 26:31-49.

Nunez PL, Srinivasan R. 2006. Electric fields of the brain: The neurophysics of EEG. New York: Oxford University Press.

Nunez PL, Wingeier BM, Silberstein RB (2001): Spatial-temporal structures of human alpha rhythms: theory, microcurrent sources, multiscale measurements, and global binding of local networks. Hum Brain Mapp 13:125-164.

Oostendorp TF, Delbeke J, Stegeman DF (2000): The conductivity of the human skull: Results of *in vivo* and *in vitro* measurements. IEEE T Biomed Eng 47:1487-1492.

Osipova D, Ahveninen J, Jensen O, Ylikoski A, Pekkonen E (2005): Altered generation of spontaneous oscillations in Alzheimer's disease. Neuroimage 27:835-841.

Osipova D, Rantanen K, Ahveninen J, Ylikoski R, Häppölä O, Strandberg T, Pekkonen E (2006): Source estimation of spontaneous MEG oscillations in mild cognitive impairment. Neurosci Lett 405:57-61.

Palmero-Soler E, Dolan K, Hadamschek V, Tass PA (2007): swLORETA: a novel approach to robust source localization and synchronization tomography. Phys Med Biol 52:1783-1800.

Parameshwaran K, Dhanasekaran M, Suppiramaniam V (2008): Amyloid beta peptides and glutamatergic synaptic dysregulation. Exp Neurol 210:7-13.

Petersen RC, Smith GE, Waring SC, Ivnik RJ, Tangalos EG, Kokmen E (1999): Mild cognitive impairment. Clinical characterization and outcome. Arch Neurol 56:303-308.

Price JL and Morris JC (1999): Tangles and plaques in nondemented aging and "preclinical" Alzheimer's disease. Ann Neurol 45:358-368.

Pritchard WS and Duke DW (1997): Segregation of the thalamic alpha rhythms from cortical alpha activity using the Savit-Green S-statistic and estimated correlation dimension. Int J Psychophysiol 26:263-271.

Richards JE (2004): Recovering dipole sources from scalp-recorded event-related-potentials using component analysis: principal component analysis and independent component analysis. Int J Psychophysiol 54:201-220.

Rombouts SA, Barkhof F, Goekoop R, Stam CJ, Scheltens P (2005): Altered resting state networks in mild cognitive impairment and mild Alzheimer's disease: an fMRI study. Hum Brain Mapp 26:231-239.

Rudelli RD, Ambler MW, Wisniewski HM (1984): Morphology and distribution of Alzheimer neuritic (senile) and amyloid plaques in striatum and diencephalon. Acta Neuropathol 64:273-281.

Sabbagh MN, Shah F, Reid RT, Sue L, Connor DJ, Peterson LK, Beach TG (2006): Pathologic and nicotinic receptor binding differences between mild cognitive impairment, Alzheimer disease, and normal aging. Arch Neurol 63:1771-1776.

Särelä J and Vigario R (2003): Overlearning in marginal distribution-based ICA: Analysis and solutions. J Mach Learn Res 4:1447-1469.

Schneider T and Neumaier A (2001): Algorithm 808: ARFIT - a matlab package for the estimation of parameters and eigenmodes of multivariate autoregressive models. ACM T Math Soft 27:58-65.

Schreckenberger M, Lange-Asschenfeldt C, Lochmann M, Mann K, Siessmeier T, Buchholz HG, Bartenstein P, Gründer G (2004): The thalamus as the generator and modulator of EEG alpha rhythm: a combined PET/EEG study with lorazepam challenge in humans. Neuroimage 22:637-644.

Schurmann M, Demiralp T, Basar E, Basar-Eroglu C (2000): Electroencephalogram alpha (8-15 Hz) responses to visual stimuli in cat cortex, thalamus, and hippocampus: a distributed alpha network?. Neurosci Lett 292:175-178.

Schwarz T (1978): Estimating the dimension of a model. Ann Stat 6:461-464.

Silva LR, Amitai Y, Connors BW (1991): Intrinsic oscillations of neocortex generated by layer 5 pyramidal neurons. Science 251:432-435.

Steriade M, Jones EG, McCormick DA. 1997. Thalamus. Netherlands: Elsevier.

Steriade M, Gloor P, Llinas RR, Lopes de Silva FH, Mesulam MM (1990a): Report of IFCN Committee on Basic Mechanisms. Basic mechanisms of cerebral rhythmic activities. Electroencephalogr Clin Neurophysiol 76:481-508.

Steriade M, Jones EG, Llinas RR. 1990b. Thalamic oscillations and signaling. New York: Wiley Interscience.

Supp GG, Schlögl A, Trujillo-Barreto N, Müller MM, Gruber T (2007): Directed cortical information flow during human object recognition: Analyzing induced EEG gamma-band responses in brain's source space. PLoS One 2:e684.

Theiler J, Eubank S, Longtin A, Galdrikian B, Farmer D (1992): Testing for nonlinearity in time series: The method of surrogate data. Physica D 58:77-94.

Trujillo-Barreto NJ, Aubert-Vazquez E, Valdes-Sosa PA (2004): Bayesian model averaging in EEG/MEG imaging. Neuroimage 21:1300-1319.

Van der Werf YD, Jolles J, Witter MP, Uylings HB (2003): Contributions of thalamic nuclei to declarative memory functioning. Cortex 39:1047-1062.

Wang K, Liang M, Wang L, Lian L, Zhang X, Li K, Jiang T (2007): Altered functional connectivity in early Alzheimer's disease: A resting-state fMRI study. Hum Brain Mapp 28:967-978.

Wang QS, Tian L, Huang YL, Qin S, He LQ, Zhou JN (2002): Olfactory identification and apolipoprotein E epsilon 4 allele in mild cognitive impairment. Brain Res 951:77-81.

Wenham PR, Price WH, Blandell G (1991): Apolipoprotein E genotyping by one-stage PCR. Lancet 337:1158-1159.

Figure legends

Figure 1. Flow chart displaying a scheme of the main analysis steps followed in this study. Note that the MVAR-EfICA methodology (represented by the inside of the dotted square line) is a combined approach using PCA, MVAR and ICA which was initially applied to the EEG datasets of the healthy old subjects to remove effects of volume conduction from multichannel EEG recordings (see Methods section). Next, significant clusters of ICA estimates were represented, identified by independent centrotypes, and located in the 3D brain space of healthy elderly and MCI patients. Finally, the directed transfer function (DTF) was applied to determine directional causal relationships between EEG-alpha sources obtained from temporal activation patterns deduced from centrotype spatial filters.

Figure 2. Analysis protocol followed to assess the significance of ICA estimates at obtaining EEG-alpha centrotypes. A. Dendrogram: The horizontal axis depicts similarity between ICA-estimates and the vertical axis denotes ICA-estimates. The points are successively joined into clusters when moving leftwards in the dendrogram. Therefore, in the leftmost partition level there is only a single cluster conveying all ICA-estimates while in the rightmost partition level each cluster contains a single ICA-estimate. According to the R-index, the best-fit partition level (marked with a vertical dashed red line) contains 10 clusters. B. ICA estimates histogram: number of ICA-estimates in each cluster at the best partition level. The number of subjects from which those ICA-estimates were found is shown in italic font within each histogram bar. Significant ICA-estimates were marked with asterisks. C. Similarity matrix: vertical and horizontal axes correspond to significant ICA-estimates in each cluster. The matrix shows the cross-similarities

values using a color scale. Clusters of ICA-estimates at the best-fit partition level are marked with red lines. Clusters 7, 9 and 10 are labeled in both the vertical and horizontal axis. Note the high intra-cluster similarities and low inter-cluster similarities that characterize those three clusters. D. ICA distribution: from top to bottom, normalized distribution of scalp potentials corresponding to the single best ICA-estimate (EEG-alpha centrotype) equivalent to clusters 7, 10 and 9.

Figure 3. Localization of electric dipole sources for the three significant EEG-alpha centrotypes. Talairach coordinates for each selected centrotype: clusters 7, caudal regions of the thalamus (x=9, y=-25, z=9); cluster 9, precuneus (x=2, y=-60, z=28); and cluster 10, cuneus (x=11, y=-97, z=13). Reconstructed EEG sources are superimposed on the corresponding sagittal MRI slices.

Figure 4. Mean activation probability of EEG-alpha sources in healthy elderly subjects and MCI patients within the lower and upper subdivisions of the alpha band. Error bars denote mean standard errors. * p < 0.005

Figure 5. Effects of normal and pathological aging on synaptic flow dynamics between EEG-alpha sources. Mean strength of the directionality (DTF) of the synaptic flow between thalamus and cortex (cuneus and precuneus) and between cortico-cortical structures involved in the generation of the lower alpha band in healthy elderly controls and MCI patients. Error bars denote mean standard errors. THAL = thalamus, CUN = cuneus, PREC = precuneus. * p < 0.008

Figure 6. Effects of age on thalamocortical synaptic flow in the upper alpha band. Scatter plot showing the degree of relationship between thalamocortical DTF values within the

upper alpha band and age in healthy elderly controls (black circles) and MCI patients (grey empty circles). The value represented for each circle results from averaging the DTF values obtained between thalamus-cuneus, thalamus-precuneus, cuneus-thalamus and precuneus-thalamus for the upper alpha band in one specific subject. The black and gray lines reflect the best fit for controls and MCI patients, respectively. Note that only healthy elderly controls showed a significant decrease of the synaptic transmission from thalamus to cortex with age.
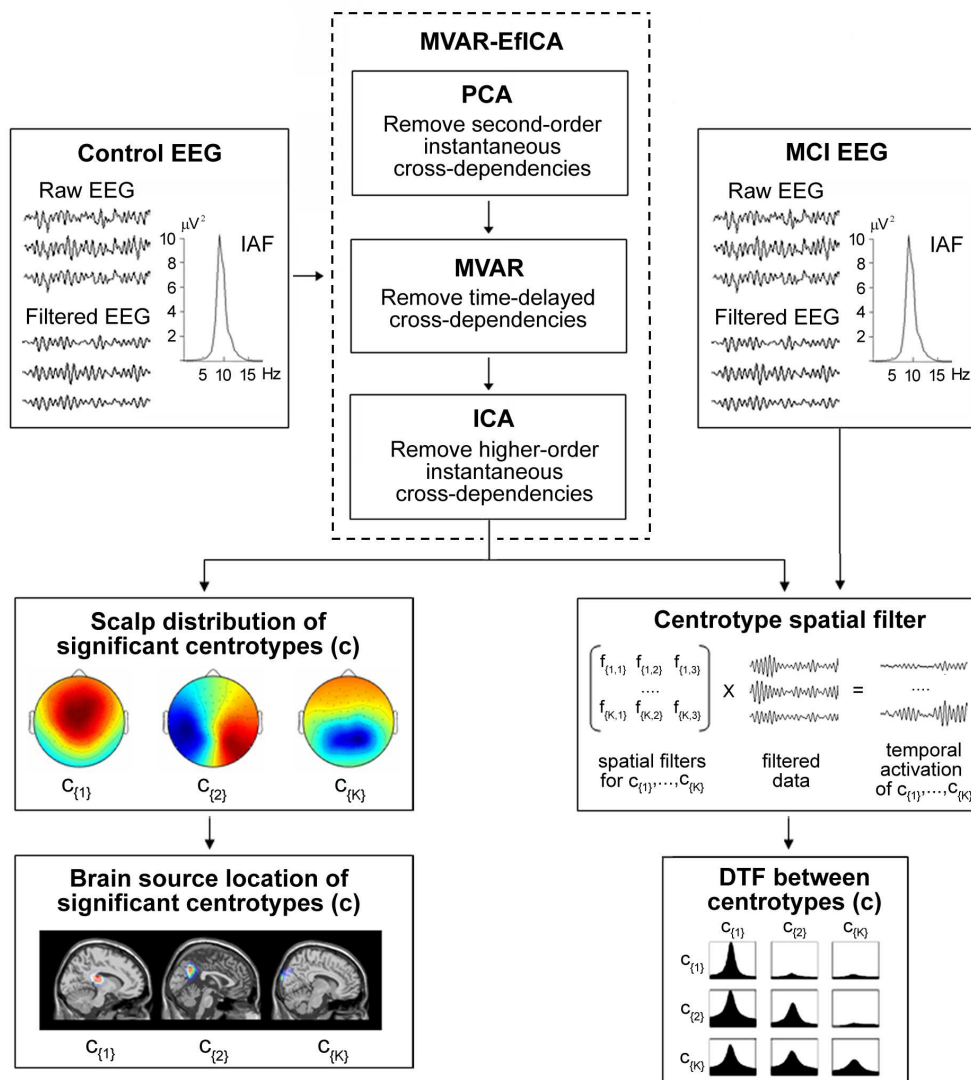
Figure 1. Flow chart displaying a scheme of the main analysis steps followed in this study. Note that the MVAR-EfICA methodology (represented by the inside of the dotted square line) is a combined approach using PCA, MVAR and ICA which was initially applied to the EEG datasets of the healthy old subjects to remove effects of volume conduction from multichannel EEG recordings (see Methods section). Next, significant clusters of ICA estimates were represented, identified by independent centrotypes, and located in the 3D brain space of healthy elderly and MCI patients. Finally, the directed transfer function (DTF) was applied to determine directional causal relationships between EEG-alpha sources obtained from temporal activation patterns deduced from centrotype spatial filters.
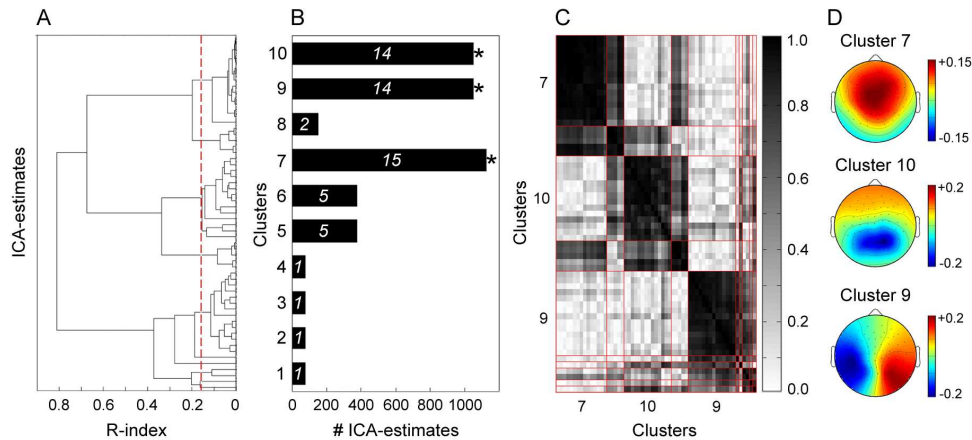160x181mm (300 x 300 DPI)

Figure 2. Analysis protocol followed to assess the significance of ICA estimates at obtaining EEG-alpha centrotypes. A. Dendrogram: The horizontal axis depicts similarity between ICA-estimates and the vertical axis denotes ICA-estimates. The points are successively joined into clusters when moving leftwards in the dendrogram. Therefore, in the leftmost partition level there is only a single cluster conveying all ICA-estimates while in the rightmost partition level each cluster contains a single ICA-estimate. According to the R-index, the best-fit partition level (marked with a vertical dashed red line) contains 10 clusters. B. ICA estimates histogram: number of ICA-estimates in each cluster at the best partition level. The number of subjects from which those ICA-estimates were found is shown in italic font within each histogram bar. Significant ICA-estimates were marked with asterisks. C. Similarity matrix: vertical and horizontal axes correspond to significant ICA-estimates in each cluster. The matrix shows the cross-similarities values using a color scale. Clusters of ICA-estimates at the best-fit partition level are marked with red lines. Clusters 7, 9 and 10 are labeled in both the vertical and horizontal axis. Note the high intra-cluster similarities and low inter-cluster similarities that characterize those three clusters. D. ICA distribution: from top to bottom, normalized distribution of scalp potentials corresponding to the single best ICA-estimate (EEG-alpha centrotype) equivalent to clusters 7, 10 and 9.
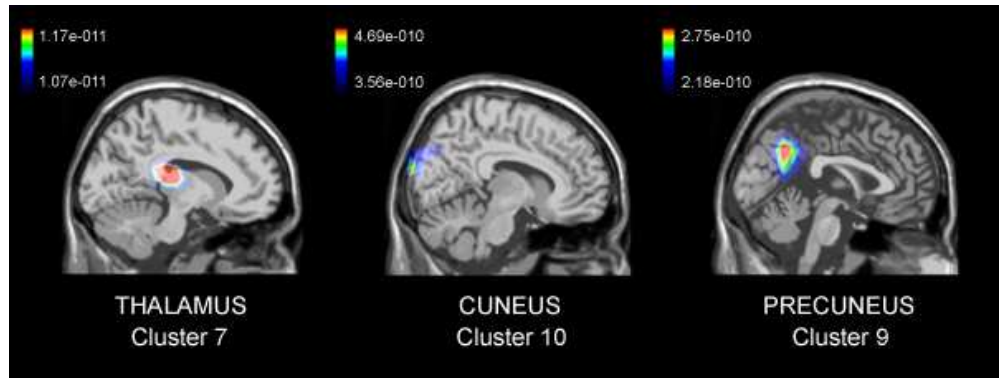160x76mm (300 x 300 DPI)

Figure 3. Localization of electric dipole sources for the three significant EEG-alpha centrotypes. Talairach coordinates for each selected centrotype: clusters 7, caudal regions of the thalamus (x=9, y=-25, z=9); cluster 9, precuneus (x=2, y=-60, z=28); and cluster 10, cuneus (x=11, y=-97, z=13). Reconstructed EEG sources are superimposed on the corresponding sagittal MRI slices. 160x60mm (96 x 96 DPI)
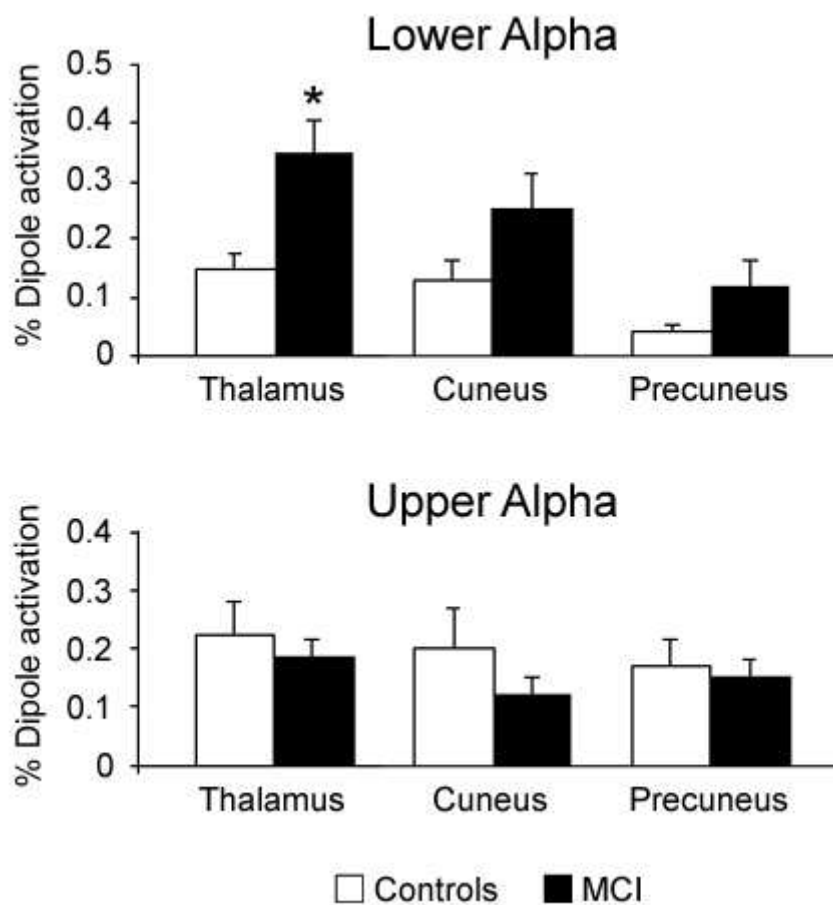
Figure 4. Mean activation probability of EEG-alpha sources in healthy elderly subjects and MCI patients within the lower and upper subdivisions of the alpha band. Error bars denote mean standard errors. * p < 0.005
79x83mm (150 x 150 DPI)
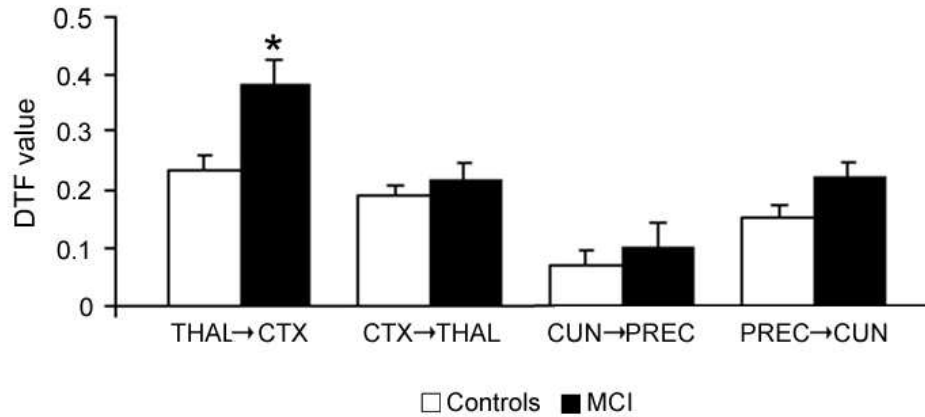
Figure 5. Effects of normal and pathological aging on synaptic flow dynamics between EEG-alpha sources. Mean strength of the directionality (DTF) of the synaptic flow between thalamus and cortex (cuneus and precuneus) and between cortico-cortical structures involved in the generation of the lower alpha band in healthy elderly controls and MCI patients. Error bars denote mean standard errors. THAL = thalamus, CUN = cuneus, PREC = precuneus. * p < 0.008
124x65mm (150 x 150 DPI)

1
2
3
4
5
6
7
8
9
10
11
12
13
14
15
16
17
18
19
20
21
22
23
24
25
26
27
28
29
30
31
32
33
34
35
36
37
38
39
40
41
42
43
44
45
46
47
48
49
50
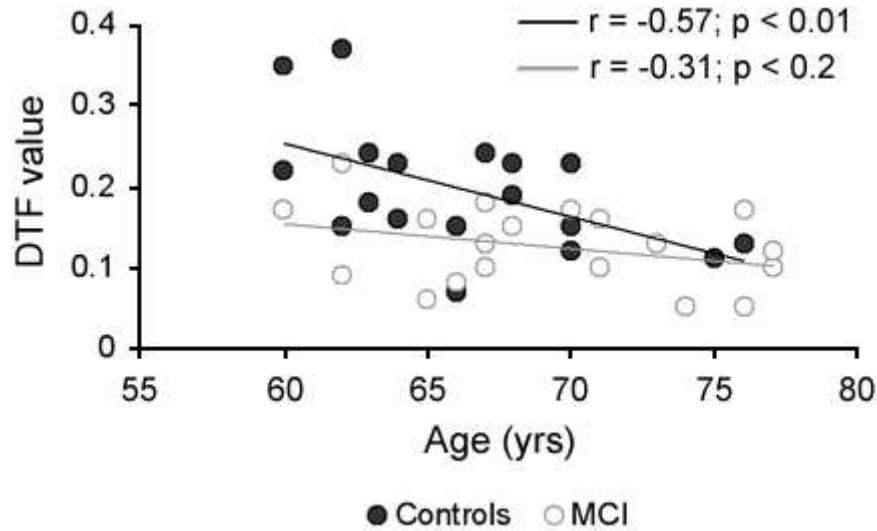51
52
53
54
55
56
57
58
59
60

Figure 6. Effects of age on thalamocortical synaptic flow in the upper alpha band. Scatter plot showing the degree of relationship between thalamocortical DTF values within the upper alpha band and age in healthy elderly controls (black circles) and MCI patients (grey empty circles). The value represented for each circle results from averaging the DTF values obtained between thalamus-cuneus, thalamus-precuneus, cuneus-thalamus and precuneus-thalamus for the upper alpha band in one specific subject. The black and gray lines reflect the best fit for controls and MCI patients, respectively. Note that only healthy elderly controls showed a significant decrease of the synaptic transmission from thalamus to cortex with age.
79x49mm (150 x 150 DPI)

TABLE 1. Subject demographics

	Controls (n = 20)	MCI (n = 20)	$P <$
Age, yr (M ± SD)	66.8 ± 4.7	68.4 ± 6.1	0.3
Gender, (F / M)	10 / 10	9 / 11	N/A
Education, yr (M ± SD)	13.5 ± 5.6	11.8 ± 6.5	0.4
MMSE (M ± SD)	28.4 ± 1.4	26.6 ± 2.7	0.01
CDR (sum of boxes)	0	0.5	N/A
Immediate recall (M ± SD)	14.4 ± 2.9	9.9 ± 2.2	10^{-5}
Delayed recall (M ± SD)	13.3 ± 2.4	6.4 ± 3.5	10^{-7}
APOE (ε_4 / non ε_4)	4 / 16	9 / 11	N/A

M ± SD (mean ± standard deviation). F (females) M (males). MMSE: Mini-Mental

State Exam, where the range from best to worst performance is 30-0. CDR: Clinical

Dementia Rating, where CDR = 0 no dementia, CDR = 0.5 questionable or very mild

dementia. N/A (not applicable).

Table 2. Means and standard errors of alpha peak frequency in healthy elderly subjects and MCI patients, carriers and non-carriers of ε4. Note that the alpha peak frequency was measured at significant centrotypes of the thalamus, cuneus, and precuneus.

Controls	9.47 ± 0.19	9.62 ± 0.18	9.57 ± 0.22
MCI			
ε4 carriers	8.67 ± 0.22	8.83 ± 0.27	9.22 ± 0.32
ε4 non-carriers	8.77 ± 0.20	9.09 ± 0.24	9.00 ± 0.29